



Laser irradiation effects on ultrafine carbon-coated LiFePO₄ using a modified solid state synthesis and olive oil as carbon source

Ghazi Ben Amor^{1,*}, Noureddine Amdouni¹, Habib Boughzala² and Jean Marc Grenèche³

¹UR Physico-Chimie des matériaux Solides, Faculté des Sciences de Tunis, Université Tunis El Manar, 1060 Tunisie

²Laboratoire de Matériaux et Cristallographie, Faculté des Sciences de Tunis, Université Tunis El Manar, 1060 Tunisie

³LUNAM, Institut des Molécules et Matériaux du Mans, UMR CNRS 6283, Université du Maine, Avenue Olivier Messiaen, 72085 Le Mans Cedex 9, France

Abstract: Nano-size LiFePO₄/C composite was synthesized via a modified solid state reaction method. Olive oil is used as carbon source. The conventional solid state process was modified by introducing two initial steps of slurry phase blending of the ingredients and solvent removal by rotary evaporation, so as to get an intimate mixing and homogenous dispersion of reactants and conductive carbon in the sample. Both structure and morphology of the LiFePO₄/C composite sample have been characterized by X-ray diffraction (XRD), Mössbauer spectrometry, transmission electron microscopy (TEM) and Raman spectroscopy. The LiFePO₄/C composite exhibited a high crystallinity. The particles of synthesized LiFePO₄/C were fine and homogeneous in size, with an average diameter of 100nm. Since the thermal effect of laser irradiation may possibly alter material surface, particular attention has been paid in characterizing the structure and component of the material surface by Raman spectroscopy. Electrochemical measurements show that the LiFePO₄/C composite cathode delivers an initial discharge capacity of 146 mAh g⁻¹ between 2.5 and 4.3V at a C/10 rate (a charger rated C/10 would return the battery capacity in 10 hours).

Keywords: LiFePO₄/C Composite; Cathode material; Lithium-ion batteries; Electrochemical performance; Modified solid state reaction.

Introduction

In recent years, lithium iron phosphate LiFePO₄ has been extensively studied as a promising cathode active material for lithium-ion batteries because of low cost, good thermal stability, low toxicity and relatively high theoretical specific capacity of 170 mAh g⁻¹ with a discharge voltage plateau of 3.5 V versus Li/Li⁺¹⁻⁵. However, one of the major problems that inhibit its use in large batteries for applications, such as hybrid electric vehicles (HEVs), is poor rate capability which can be attributed to its intrinsically low electronic conductivity⁶ and lithium-ion diffusivity^{1,7} at room temperature. LiFePO₄ optimization for good electrochemical performances in lithium-ion batteries has been achieved in controlling of synthetic parameters to adjust particle size and morphology to reduce the transport path length of Li⁺⁸⁻¹¹ and/or in

*Corresponding author : Ghazi Ben Amor

Email address : ghazghouzi@yahoo.fr

DOI : <http://dx.doi.org/10.13171/mjc.3.5.2014.11.08.10.36/ghazi>

forming an electronic conductive particles coating to provide a pathway for electron transfer¹²⁻¹⁶. Thin carbon layer coating on the LiFePO₄ particles is one of the most promising ways to enhance electrochemical properties of LiFePO₄. Doeff et al.¹⁷ reported that the morphology and the characteristics of residual carbon can affect the electrochemical performance of LiFePO₄. To obtain LiFePO₄ with fine particles and an intimate carbon coating for high power purpose, many soft chemistry routes, such as sol-gel synthesis¹⁸, co-precipitation¹⁹, hydrothermal reaction^{20,21}, and emulsion-drying method²², have been tested. These methods often suffer from long synthesis time, low production rate, generation of large chemical and aqueous wastes, and requirement of an additional high-temperature sintering step to enhance crystallinity²³. For the high temperature solid-state route used for the synthesis of LiFePO₄^{8,14,24-30}, results in a final product are frequently composed of impurities like Li₃Fe₂(PO₄)₃, Fe₂O₃ and Li₃PO₄, and it is also very difficult by such process to obtain fine and homogeneous particle that is regarded as a key factor for the power ability.

In this work, we adopted high temperature solid-state method with a modified protocol for the synthesis of LiFePO₄/C composite, olive oil was used as carbon source. Structural characteristics of the synthesized compounds are described by XRD, ⁵⁷Fe Mössbauer spectrometry, TEM and Raman micro-spectrometry analysis. Galinetto et al.³¹ studied the effect of laser irradiation on the thermal stability of LiFePO₄. They have concluded that its stability up on laser irradiation depends on the synthesis route, or more specifically, on the grain size and degree of order of the olivine structure. Ramana et al.³² pointed out the possibility of the photodecomposition of LiFePO₄ samples and used an excitation laser power lower than 10 mW to prevent the destruction of the samples. In this way, the effects of laser beam power on our synthesized LiFePO₄/C particles were investigated.

Experimental Section

Synthesis of samples

For the preparation of LiFePO₄ powder, the reactants (FeC₂O₄·2H₂O, Li₂CO₃ and NH₄H₂PO₄ in a ratio of Li: Fe: P = 1:1:1) were mixed thoroughly with high purity ethanol and were stirred under high purity argon for 24h. Ethanol was eliminated by using a rotary evaporator. Thermal treatment was performed in two stages under high purity argon flow. The precursor powders were first heated at 350°C for 3h in order to drive away the gases and to initiate the synthesis, then reground and annealed at 700°C for 10h. The sample obtained in this manner is hereafter named LFP. For LiFePO₄/C composite, the olive oil as a carbon source was added to the mixture of the starting materials after elimination of ethanol. During the calcinations, olive oil was carbonized and the produced carbon was coated on surface of the LiFePO₄ particles. The final product is referred to LFP/C sample in this work.

Structural and morphological characterization

The crystalline phase of the particles was investigated with X-ray diffraction using a Philips X'Pert PRO diffractometer equipped with a Cu anticathode at room temperature. The Rietveld refinement of the X-ray powder diffraction pattern was performed using TOPAS 4.2 to obtain the crystal structure parameters. Mössbauer spectroscopy measurements were performed in transmission geometry at 300 K, in plastic sample holders, using a constant-acceleration spectrometer with a ⁵⁷Co source. Calibration was achieved from a standard α -iron foil at room temperature (300K). The spectra were analyzed using the MOSFIT program³³ which is based on non-linear least squares fitting procedures assuming Lorentzian Mössbauer lines and the values of isomer shift are quoted relative to that of α -Fe at 300K. Micro-structural observation

was performed using an analytical transmission electron microscope FEI Tecnai G2 operating at 200 kV with a LaB₆ filament. Specific surface area of LiFePO₄/C sample was determined from the N₂ adsorption isotherms at 77K with the BET method using a Micromeritics ASAP 2020 Analyzer. The carbon amount was determined with a CHNO/S analyzer (2400II, PerkinElmer). Raman spectra of the samples were recorded at room temperature in the backscattering configuration on a T64000 Jobin-Yvon (Horiba) spectrometer under a microscope with a 100X objective focusing the 514nm line from an Ar-Kr ion laser (Coherent, Innova). Measurements using different laser output powers between 50 and 300 mW (corresponding to a laser power of 2 and 25 mW on the sample) were carried out consecutively without moving the sample. Single spectra were recorded twice with an integration time of 20 s.

The electrode used for testing the electrochemical performance was manufactured by mixing 75 wt. % LiFePO₄, 20 wt. % carbon black and 5 wt. % polyvinylidene difluoride. The intensively mixed slurry was rolled into a sheet, and then cut into pellet and dried at 60°C for 12h. The performance of the LiFePO₄ cathode was evaluated by Swagelok type cell, using a lithium metal as both the reference and the anode electrode. A borosilicate glass fiber sheet saturated with electrolyte was used as separator, the electrolyte used consisted of a 1 M solution of LiClO₄ in a mixed (1:1) solvents of ethylene carbonate (EC) and dimethyl carbonate (DMC). The cell assembly was performed in an argon atmosphere glove box model JACOMEX. The cells were tested between 2.5 V and 4.3 V at C/10 rate at ambient temperature.

Results and Discussion

The X-ray patterns of LFP and LFP/C samples obtained by the modified solid state preparation are reported in Figure 1. All diffraction peaks can be attributed to an ordered olivine LiFePO₄ structure with orthorhombic lattice (*Pnma*).

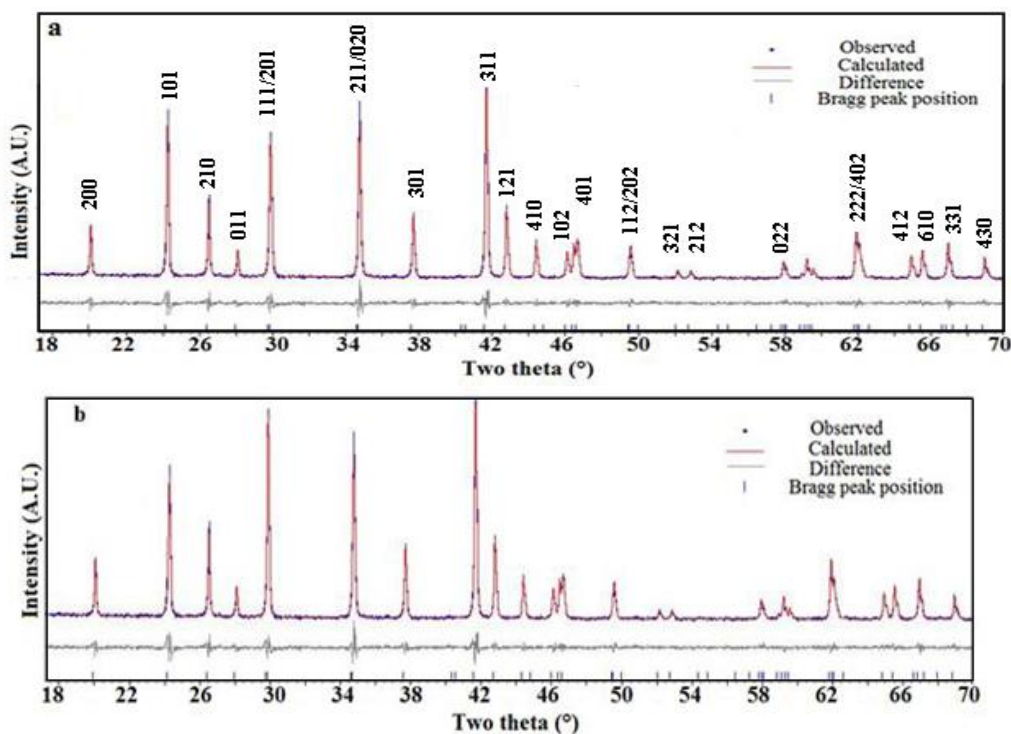


Figure 1. Rietveld refinement on the XRD pattern of (a) bare LiFePO₄ (LFP) and (b) LFP/C.

The cell parameter values of LFP and LFP/C samples calculated from the XRD patterns based on the *Pnma* space group are listed in Table 1. The lattice parameters are in agreement with the A.S.T.M. (American Society for Testing Materials) data³⁴. The sharp peaks indicate a good crystallinity³⁵. An efficient criterion for the crystal quality is the unit cell volume which must be in the range [291.0-291.5] Å³ for LiFePO₄³⁶. There is no evidence for the formation of crystalline or amorphous carbons. Figure 1b and Table 2 show the Rietveld refinement results of the XRD pattern of the LFP/C composite. The observed and calculated patterns match very well ($R_{\text{Bragg}} = 0.399$).

Table 1: Lattice parameters deduced from the analysis of X-ray diffraction pattern for LFP and LFP/C

Sample	LFP	LFP/C	ASTM. [34]
<i>a</i> (Å)	10.328(25)	10.330(23)	10.330
<i>b</i> (Å)	6.007(14)	6.009(12)	6.010
<i>c</i> (Å)	4.695(13)	4.694(12)	4.692
<i>V</i> (Å ³)	291.3(3)	291.3(11)	291.3

Noticeable structural changes were not observed in the XRD pattern of the carbon-coated LiFePO₄ indicating that the olivine structure was well maintained after carbon coating. Impurity phases such as Fe₂O₃ and Li₃Fe₂(PO₄)₃ that usually appear in LiFePO₄ products synthesized by solid-state reaction were not observed in the carbon-coated LiFePO₄. The carbon in the composite prevents the oxidation of iron from Fe²⁺ into Fe³⁺, which hinders the appearance of impurity, and stops the growth of the LiFePO₄ particle³⁷. However, Yamada et al. observed small Fe³⁺ impurity using Mössbauer spectroscopy³⁸ more sensitive than X-ray diffraction to detect Fe³⁺ impurities.

Table 2: Structural data and Rietveld refinement parameters of LFP/C composite

Structure						
Phase formula		LFP/C	Space group			Pnma
<i>a</i> (Å)		10.330(23)	Cell Mass			631.036
<i>b</i> (Å)		6.009(12)				
<i>c</i> (Å)		4.694(12)	Crystallite size (nm)		120 (50)	
Cell Volume(Å ³)		291.3(11)	Crystal Density (gcm ⁻³)		3.597(2)	
Site	Np	x	y	z	Occ.	B _{eq}
Li	4	0.000	0.000	0.000	1	1
Fe	4	0.284(22)	0.250	0.976(69)	1	1
P	4	0.097(45)	0.250	0.418(88)	1	1
O1	4	0.096(13)	0.250	0.745(19)	1	1
O2	4	0.456(12)	0.250	0.202(24)	1	1
O3	8	0.166(99)	0.043(13)	0.286(17)	1	1

The Mössbauer spectra for LiFePO₄ crystals have been measured by some researchers³⁸⁻⁴⁰ and the values of isomer shift δ and quadrupole splitting Δ have been reported ($\delta = 1.20$ - 1.22 mm/s and $\Delta = 2.95$ - 2.98 mm/s). The ⁵⁷Fe Mössbauer spectrum of the prepared LFP/C recorded at room temperature is illustrated in Figure 2 and the results indicate only one quadruple doublet. The mean values of the hyperfine parameters ($\delta = 1.23$ mm/s and $\Delta = 2.96$ mm/s) are assigned to Fe²⁺ ions with a high spin configuration of 3d electrons and the asymmetric local

environment at the Fe in LiFePO₄ as explained by Yamada et al.³⁸, the low line width $\Gamma = 0.34$ mm/s value is due to the formation of LiFePO₄ crystals. We note the absence of Fe³⁺, any incidence of Fe³⁺ would result in a weak and closely spaced doublet located in between the very strong Fe²⁺ peaks of the doublet, as it was observed in the work of Prince et al.³⁹.

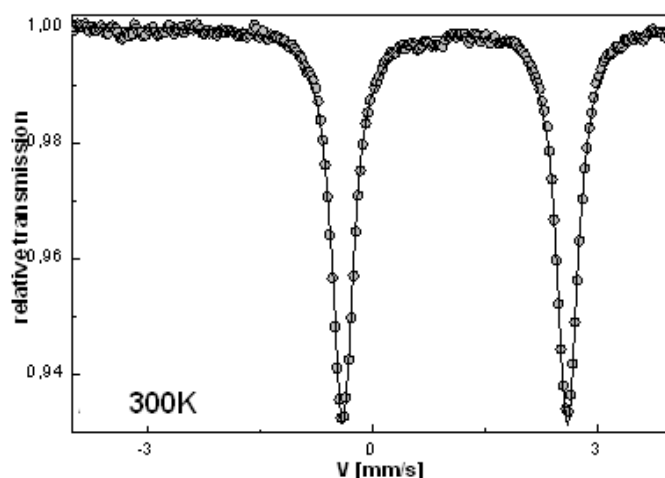


Figure 2. Mössbauer spectrum of the synthesized LFP/C.

The TEM image of the nanocrystals synthesized in the absence of organic molecules displayed spherical and polygonal particles ranging from 150 to 200 nm (Fig. 3a). This small particle size has not been reported yet for solid state reaction. The unique morphology and size are due to the homogenization of the starting material by stirring in ethanol for several hours. The particles size was decreased with the addition of olive oil into the reaction system as illustrated in Figure 3b. The nanocrystals displayed uniform and spherical particles ranging from 50 to 150 nm. We note the presence of small extensions at the surface of the LFP/C particles. Both morphology and size of LFP/C composite are due to the very intimate mixing of the reactants on the molecular level by stirring in ethanol and to the admixing of olive oil in the starting material. Note that the average particle size of the synthesized LFP/C sample is consistent with the obtained crystal grain size calculated from XRD pattern, implying that the particles are not formed from the agglomeration of several grains. Thus, it is seen that the modifications introduced in this study result in attaining much smaller particles with a narrow size range. This indicates that compared to the conventional process, the modified process leads to (1) an intimate blending of the ingredients resulting in a more uniform particle size, and (2) a more homogenous distribution of carbon source throughout the sample that limits the particle growth effectively. TEM also reveals that the particles have a rough surface without sharp edges; an added indication of the efficient carbon coating achieved. The results indicate that the addition of carbon is beneficial to the control of the particle size. The characteristics of the LFP and LFP/C powders are listed in Table 3.

Table 3: Characteristics of the LFP and LFP/C powders.

Olivine powder	Carbon content (wt%)	BET surface area (m ² g ⁻¹)	Particles size (nm) by XRD
LFP	-	6	150-200
LFP/C	3.84	34	50-150

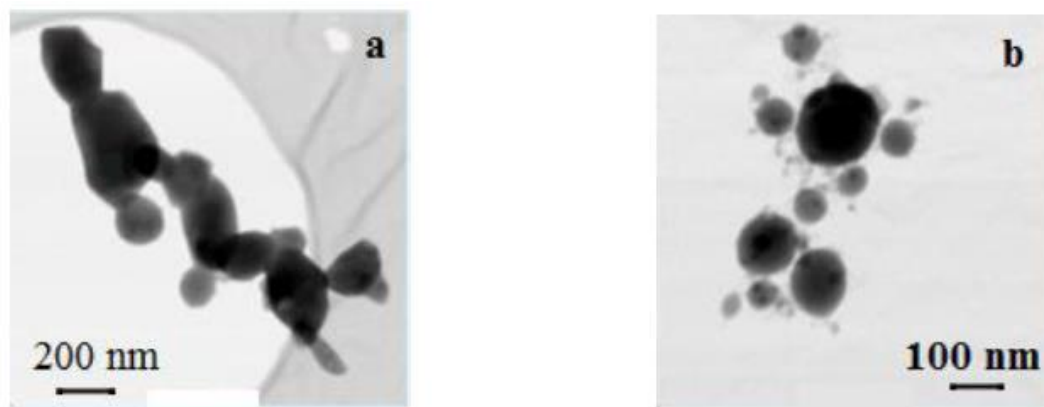


Figure 3. TEM observation bright-field images of the prepared powders: (a) LFP and (b) LFP/C.

Raman spectroscopy is sensitive to the surface of materials compared with XRD; this technique allows the detection of impurity phases even when their amount is well below the detectable limit of XRD. Phospho-olivines are Raman active compounds⁴¹⁻⁴⁴. Figure 4 displays the Raman spectra of the LFP powder. .

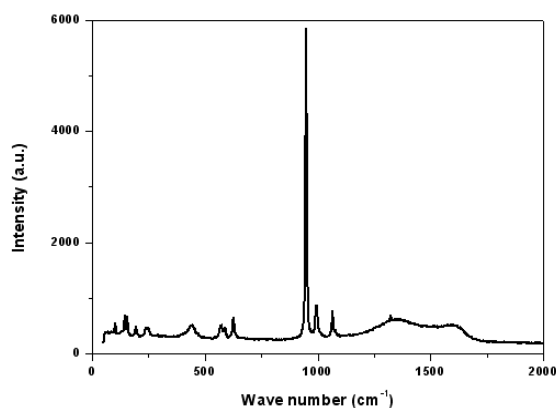


Figure 4. Raman spectrum of LFP sample.

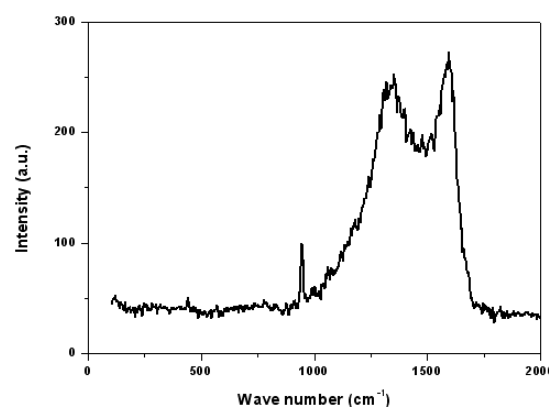


Figure 5. Raman spectrum of LFP/C sample

To exclude the influence of laser heating which can induce phase transformations thus preventing a real phase homogeneity characterization, Raman spectrum was collected under moderate laser power of 10 mW. The peaks observed agree very well to the assignments reported in the literature^{41,45}. No evidence of impurity such as iron oxide was seen in the Raman spectra. The LFP material demonstrates a sharp peak near 949 cm^{-1} , suggesting a high degree of order. The broad bands at 1355 and 1596 cm^{-1} are well known from the spectroscopy of carbon as being the D and G bands that originate from amorphous and graphitic forms, respectively. However the presence of the latter was only a few times observed. Such carbon contaminations were also reported by both Song et al.⁴⁶ on their one step made LiFePO_4 thin films and Hu et al.⁴⁷ on their sol-gel made LiFePO_4 powder. The former groups ascribed its presence to its preparation that enlisted a decomposition of metallo-organic precursors

Raman spectrum of LFP/C sample is depicted in Figure 5. The carbon layer that blocked off the signals from LiFePO_4 to a certain extent in the measurement makes it difficult to see the details of the spectrum of the olivine structure due to the attenuation of the signal and the overlapping of the spectral bands. Only a weak signal at 945 cm^{-1} related to PO_4^{3-} anion symmetric stretching (the strongest peak in the olivine LFP spectrum) is observed. Typical D

and G bands of carbon appear around 1351 and 1596 cm^{-1} . When analyzing carbonaceous materials, G band (1596 cm^{-1}) is assigned to the E_{2g} graphite mode, and D band (1351 cm^{-1}) is associated to A_{1g} mode, that is related to the breaking of symmetry occurring at the edges of graphite sheets⁴⁸⁻⁴⁹. Doeff et al.⁵⁰⁻⁵¹ pointed out that the ratio of the disordered/graphene (D/G) of the *in situ* carbon coating formed from the carbon-containing precursor strongly affected the electrochemical performance of LiFePO_4 . The carbon coating with lower D/G ratios outperformed those with higher D/G ratios. A small I_D/I_G intensity ratio of 0.93 for LFP/C reveals decreased level of disorder⁵⁰. The result suggests an improved electronic conductivity of this sample which could be beneficial to improve the electrochemical properties and indicates that the olive oil can be pyrolyzed to form highly graphitized carbon with low I_D/I_G ratio and good electronic properties⁵⁰.

The power setting of the excitation laser should be carefully controlled in Raman spectroscopy measurements. Raman spectra of LFP/C were collected as a function of laser power and are presented in Figure 6. The irradiated region has the olivine structure, as clearly evidenced by the main peak at around 945 cm^{-1} . The olivine phase is stable in the LFP/C sample after high irradiation laser power. The intensities of the vibrational peaks of C-coated LiFePO_4 enhanced markedly as the laser power increased. The resulting Raman spectrum can no longer be associated with a pure olivine-coated structure; two intense bands at about 217 and 277 cm^{-1} are present and are due to the formation of the hematite phase. The presence of hematite clusters during Raman inspection of the sample is favored by the reduced grain size^{52,53} and so by the high specific surface area; the specific area value obtained by BET surface analysis was 34 m^2g^{-1} for LFP/C sample. These bands are related to A_{1g} and E_g vibrations in $\alpha\text{-Fe}_2\text{O}_3$ ⁵⁴⁻⁶¹. Xia et al., with the use of Raman spectroscopy, showed that the exposure of LiFePO_4 in hot air leads to the formation of $\alpha\text{-Fe}_2\text{O}_3$, lithium and iron phosphates on the surface of the samples⁶².

The Raman spectra in Figure 6 show that the sample is able to dissipate the thermal energy and strain accumulated from the laser irradiation even when the laser power reaches 300 mW. As reported by previous researchers, the ability to accommodate stress is better for small particles than for large grains⁶³. The effectiveness of laser irradiation depends on the grain size and degree of order of the olivine structure: the more ordered the structure, the less effective the transformation.

So, the grain size of LFP/C explains the stabilization of the general spectra under laser irradiation. The strong thermal endurance of the LFP/C material is ascribed to the high thermal conductivity after carbon coating; with high thermal conductivity, it is not easy to accumulate heat and lattice strain. Generally speaking, owing to the absorption of radiation in the confocal micro-Raman setup, the local temperature may increase by hundreds of degrees, inducing the wavenumber shift of Raman modes, or even the sample alteration as the result of oxidation, recrystallization, order-disorder transitions, phase transition or decomposition⁶³. Figure 7 shows the characteristic vibration near 945 cm^{-1} which experienced a red shift and line broadening; signifying changes in the nature of this sample but the olivine crystal structure is not destroyed when the power reached 300 mW.

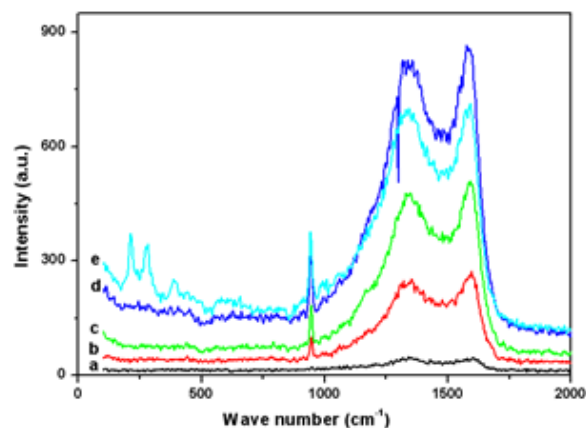


Figure 6. Raman spectra of LFP/C sample obtained at different laser power levels: (a) 10 mW; (b) 50 mW; (c) 100 mW; (d) 200 mW and (e) 300 mW.

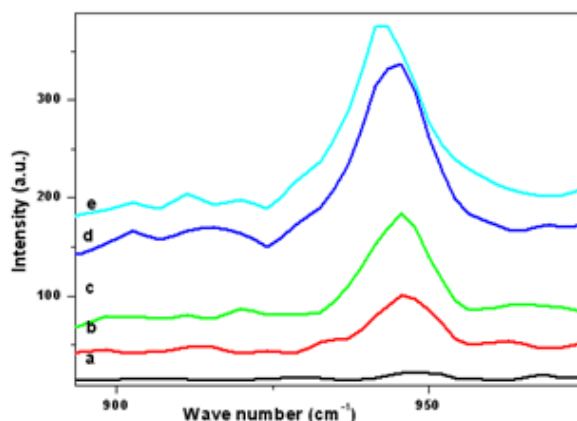


Figure 7. Evolution of the vibrational peak centered near 945 cm^{-1} for the LFP/C sample at different laser power levels: (a) 10 mW; (b) 50 mW; (c) 100 mW; (d) 200 mW and (e) 300 mW.

Markevich et al.⁶⁴ investigated effects of laser irradiation power on the Raman spectra of LiFePO_4/C powder in the ambient atmosphere at a moderate laser power, the phenomenon of the removal of the carbon coating layer was detected. LiFePO_4/C powder, with carbon layer gasification, undergoes oxidative decomposition by the oxygen with the formation of $\text{Li}_3\text{Fe}_2(\text{PO}_4)_3$ and $\alpha\text{-Fe}_2\text{O}_3$, even at a moderate power of the excitation laser. A completely different type of situation occurs in the case of LFP/C; full gasification of carbon does not occur, even at a laser power of 300 mW during the spectrum acquisition. It is clear that during the exposure of the sample to the laser beam, the ratio of intensities of the bands related to carbon and the olivine band at 945 cm^{-1} changes slightly, especially for a laser irradiation power under 200 mW; the carbon coating layer is not removed from the surface of particles, the peaks with a lower intensity related to the olivine structure do not appear as the laser power is increased. This phenomenon can be explained by the fact that olive oil is soap and can favorably interact with LiFePO_4 regardless of its various properties; the raw materials of soaps are fatty acids or surfactants and the main ingredients of olive oil are fatty acids.

Electrochemical performance of the LFP/C was examined by charge discharge tests. Franger et al.⁶⁵ reported that the specific capacity is very dependent on the particle size. The carbon coating on the LiFePO_4 surface does not only increase the electronic conductivity via carbon on the surface of particles, but also enhances the ion mobility of lithium ion due to prohibiting the grain growth during post-heat-treatment. Figure 8 illustrates the charge/discharge voltage profiles for a LFP/C electrode at the C/10 rate. A flat voltage plateau was observed at the potential of 3.5 V versus Li/Li^+ . This electrochemical behavior corresponds to the solid-state redox of $\text{Fe}^{2+/3+}$ in the LiFePO_4 accompanying with Li^+ ion extraction and insertion¹. The LiFePO_4/C composite cathode delivers an initial discharge capacity of 146 mAh g^{-1} between 2.5 and 4.3V. The smaller particle size, which is helpful for accessibility of the redox centers, is favorable to achieve larger capacity. During synthesis, the olive oil particles limit the growth of large crystallites, possibly by segregating the crystalline seeds, favoring their dispersion and homogenizing their size. This leads to an increase of the specific surface area measured by the BET method ($34\text{ m}^2\text{ g}^{-1}$) and it makes the electrolyte accessible to a more extended region of the active material. According to Padhi et al.¹, the surface area (i.e., particle

size) is a critical factor in determining the cell performance of LiFePO_4 , because the charge–discharge process is controlled by lithium transport across the $\text{LiFePO}_4/\text{FePO}_4$ interface.

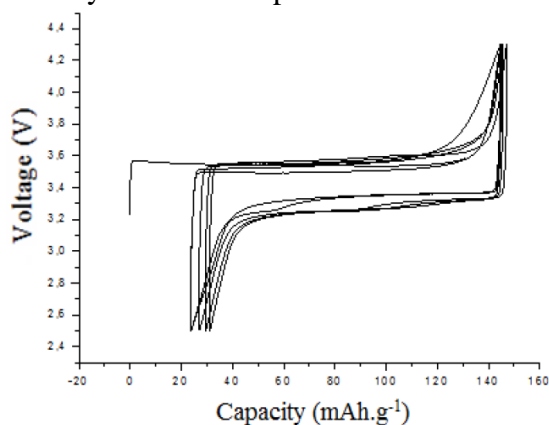


Figure 8. Charge–discharge curves of the LFP/C electrode.

Conclusions

Pure and well-crystallized LiFePO_4/C composite with small particle size was synthesized using olive oil as a carbon source by modified protocol of high temperature solid-state method. This coating was effective in enhancing capacity, LiFePO_4 coated with olive oil as a carbon source can deliver first discharge capacity of 146 mAh g^{-1} at a C/10 rate. The use of olive oil as a carbon source prevents the particle growth during the final sintering process and provides narrow particle size distribution and better homogeneity of the carbon coating. By adopting a relatively high temperature solid-state method as described and a using of olive oil as carbon source, it is possible to synthesize cathode materials on nano-scales that could accomplish high capacity.

Raman spectra of the synthesized LiFePO_4/C as a function of different Ar-Kr laser power revealed that this composite possesses a good stability under various laser power irradiations. Particular attention has to be paid when using the micro-Raman technique for the characterization of the LiFePO_4 system. Phase transformation can be induced when the laser beam is focused on a spot with a diameter of only a few micrometers, exposure of olivine coated- LiFePO_4/C with olive oil as carbon source at 300 mW power of a 532-nm laser is not sufficient to destroy the crystal structure of the obtained compound. C-coated LiFePO_4 exhibits a high thermal stability and a strong thermal endurance, which are attributed to the enhanced thermal conductivity after the carbon coating. The phenomenon of the removal of the carbon coating layer is not observed and the olivine structure of LiFePO_4/C powder remains unchanged. This phenomenon can be explained by the fact that olive oil is soap and can favorably interact with LiFePO_4 regardless of its various properties; the raw materials of soaps are fatty acids or surfactants and the main ingredients of olive oil are fatty acids.

Further efforts on the carbon coating status correlated with the carbon content are underway in our group.

References

- 1- A.K. Padhi, K.S. Nanjundaswamy, J.B. Goodenough, *J. Electrochem. Soc.*, **1997**, 144, 1188.
- 2- A.S. Andersson, J.O. Thomas, *J. Power Sources*, **2001**, 97-98, 498.

- 3- D.D. MacNeil, Z. Lu, Z. Chen, J.R. Dahn, J. Power Sources, **2002**, 108, 8.
- 4- M. Takahashi, S.I. Tobishima, K. Takei, Y. Sakurai, Solid State Ionics, **2002**, 148, 283.
- 5- S. Scaccia, M. Carewska, P. Wisniewski, P.P. Prosini, Mater. Res. Bull., **2003**, 38, 1155.
- 6- S.Y. Chung, J.T. Bloking, Y.M. Chiang, Nat. Mater., **2002**, 1, 123–128.
- 7- P.P. Prosini, M. Lisi, D. Zane, M. Pasquali, Solid State Ionics, **2002**, 148, 45-51
- 8- A. Yamada, S.C. Chung, K. Hinokuma, J. Electrochem. Soc., **2001**, 148, A224.
- 9- Delacourt, C., Poizot, P., Levasseur, S. & Masquelier, *Electrochem. Solid State Lett.*, **2006**, 9, A352- A355.
- 10- Wang L., Huang Y.D., Jiang R.R., and Jia D.Z., *Electrochim. Acta*, **2007**, 52, 6778.
- 11- J. Xiao, W. Xu, D.W. Choi, J.G. Zhang, J. Electrochem. Soc., **2010**, 157, A142.
- 12- N. Ravet, Y. Chouinard, J.F. Magnan, S. Besner, M. Gauthier, M. Armand, Journal of Power Sources, **2001**, 97, 503 Special Iss. SI.
- 13- S.F. Yang, P.Y. Zavalij, M.S. Whittingham, Electrochemistry Communications, **2001**, 3, 505.
- 14- S. Franger, F. Le Cras, C. Bourbon, H. Rouault, Journal of Power Sources, **2003**, 119, 252.
- 15- C.M. Doherty, R.A. Caruso, B.M. Smarsly, P. Adelhelm, C.J. Drummond, Chem. Mater., **2009**, 21, 5300.
- 16- Y. Yu, L. Gu, C.B. Zhu, P.A. van Aken, J. Maier, J. Am. Chem. Soc., **2009**, 131, 15984.
- 17- M. Doeff, Y. Hu, F. McLarnon, R. Kostecki, Electrochem. Solid State Lett., **2003**, 6 A207.
- 18- M. Piana, B.L. Cushing, J.B. Goodenough, N. Penazzi, Solid State Ionics, **2004**, 175, 233.
- 19- P.P. Prosini, M. Carewska, S. Scaccia, P. Wisniewski, S. Passerini, M. Pasquali, J. Electrochem. Soc., **2002**, 149, A886.
- 20- S. Tajimi, Y. Ikeda, K. Uematsu, K. Toda, M. Sato, Solid State Ionics, **2004**, 175, 287.
- 21- K. Dokko, S. Koizumi, K. Shiraishi, K. Kanamura, J. Power Sources, **2007**, 165, 656.
- 22- T.H. Cho, H.T. Chung, J. Power Sources, **2004**, 133, 272.
- 23- S. Hong, S. J. Kim, J. Kima, K. Y. Chung, B. Chob, J. W. Kang, J. of Supercritical Fluids, **2011**, 55, 1027–1037
- 24- A.K. Padhi, K.S. Nanjundaswamy, C. Masquelier, S. Okada, J.B. Goodenough, J. Electrochem. Soc., **1997**, 144, 1609–1613.
- 25- D.Wang, X.Wu, Yh.Wang, L. Chen, J. Power Sources, **2005**, 140, 125.
- 26- M.Koltypin, D.Aurbach, L.Nazar,B. Ellis, J. Power Sources, **2007**, 174, 1241.
- 27- N. J. Yun, H. W. Ha, K.H. Jeong, H. Y. Park, K. Kim, J. Power Sources, **2006**, 160, 1361.
- 28- M. Takahashi, Sh. Tobishima, K. Takei, Y. Sakurai, J. Power Sources, **2001**, 97, 508.
- 29- G. Ting-Kuo Fey, T.-L. Lu, J. Power Sources, **2008**, 178, 807.
- 30- K. Zaghbi, N. Ravet, M. Gauthier, F. Gendron, A. Mauger, J.B. Goodenough, C.M. Julien, J.Power Sources, **2006**, 163, 560.
- 31- P. Galinetto, M.C. Mozzati, M.S. Grandi, M. Bini, D.Capsoni, S. Ferrari, V. Massarotti, J.Raman Spectrosc., **2010**, 41, 1276–1282.
- 32- C. Ramana, A. Mauger, F. Gendron, C. Julien, K. Zaghbi, J. Power Sources, **2009**, 187, 555-564.
- 33- J. Teillet, F. Varret, MosfitProgramm, University du Maine, unpublished, **1976**.
- 34- Two X-ray Powder Diffraction Data Files are reported by A.S.T.M. (American Society for Testing Materials) for LiFePO₄. Our own data fit those of ref. 81-1173.

- 35- K. Rissouli, K. Benkhoucha, J.R. Ramos-Barrado, C. Julien, Mater. Sci. Eng., **2003**, B 98, 185
- 36- J. J. Chen, M. S. Whittingham, Electrochemistry Communications, **2006**, 8, 855-858.
- 37- R. Dominko, M. Bele, M. Gaberscek, M. Remskar, et al., J. Electrochem.Soc., **2005**, 152, A607-A610.
- 38- A. Yamada, S.C. Chung, K. Hinokuma, J. Electrochem. Soc., **2001**, 148, A224.
- 39- A.A.M. Prince, S. Mylswamy, T.S. Chan, R.S. Liu, B. Hannoyer, M. Jean, C.H. Shen, S.M. Huang, J.F. Lee, G.X. Wang, Solid State Commun., **2004**, 132, 455.
- 40- M.A.E. Sanchez, G.E.S. Brito, M.C.A. Fantini, G.F. Goya, J.R. Matos, Solid State Ionics, **2006**, 177, 497.
- 41- C. Burba, R. Frech, J. Electrochem. Soc., **2004**, 151, A1032–A1038.
- 42- C. Burba, R. Frech, Spectrochim. Acta A, **2006**, 65, 44–50.
- 43- C. Julien, A. Mauger, A. Ait-Salah, M. Massot, F. Gendron, K. Zaghib, Ionics, **2007**, 13, 395-411.
- 44- C. Ramana, A. Mauger, F. Gendron, C. Julien, K. Zaghib, J. Power Sources, **2009**, 187, 555-564.
- 45- W. Paraguassu, P. T. C. Freire, V. Lemos, S. M. Lala, L. A. Montoro and J. M. Rosolen, J.Raman Spectrosc., **2005**, 36, 213–220.
- 46- S.W. Song, R.P. Reade, R. Kosteckki, K.A. Striebel, J. Electrochem. Soc., **2006**, 153 (1), A12.
- 47- Y. Hu, M.M. Doeff, R. Kosteckki, R. Fiñones, J. Electrochem. Soc., **2004**, 151 (8), A1279.
- 48- F. Tunistra, J.L. Koenig, J. Chem. Phys., **1970**, 53, 1126.
- 49- D.S. Night, W.B. White, J. Mater. Res., **1989**, 4, 385.
- 50- M.M. Doeff, Y. Hu, F. McLarnon, R. Kosteckki, Electrochem. Solid State Lett., **2003**, 6, A207.
- 51- M.M. Doeff, J.D. Wilcox, R.Kosteckki, G. Lau, J. Power Sources, **2006**, 163, 180-184.
- 52- M.Bini, M.C.Mozzati, P.Galinetto, D.Capsoni, S.Ferrari, M. S.Grandi, V. Massarotti, J. Solid State Chem., **2009**, 182, 1972.
- 53- I. V. Chernyshova, M. F. Hochella Jr, A. S. Madden, Phys.Chem., **2007**, 9, 1736.
- 54- A. Zoppi, C. Lofrumento, E. Castellucci, C. Dejoie, Ph. Sciau, J. Raman Spectrosc. 37, **2006**, 1131–1138.
- 55- P. Lottici, C. Baratto, D. Bersani, G. Antonioli, A. Montenero, M. Guarneri, Opt. Mater., **1998**, 9, 368-372.
- 56- L. Wan, K. Shi, X. Tian, H. Fu, J. Solid State Chem., **2008**, 181, 735-740.
- 57- C.P. Leon, L. Kador, M. Zhang, A.H.E. Muller, J. Raman Spectrosc., **2004**, 35, 165-169.
- 58- S. Azuma, M. Sato, Y. Fujimaki, S. Uchida, Y. Tanabe, E. Hanamura, Phys. Rev.B, **2005**, 71, 014429.
- 59- K.F. McCarty, Solid State Commun., **1988**, 68, 799–802.
- 60- M. Massey, U. Baier, R. Merlin, W. Weber, Phys. Rev.B, **1990**, 41, 7822-7827.
- 61- D. Bersani, P. Lottici, A. Montenero, J. Raman Spectrosc., **1999**, 30, 355-360.
- 62- X.Xia, Z.Wang, L.Chen, Electrochem. Commun., **2008**, 10, 1442-1444.
- 63- O. N. Shebanova, P. Lazor, J. Raman Spectrosc., **2003**, 34, 845.
- 64- E. Markevich, R. Sharabi, O. Haik, V. Borgel, G. Salitra, D. Aurbach, G. Semrau, M.A. Schmidt, N. Schall, C. Stinner, Journal of Power Sources, **2011**, 196, 6433.
- 65- S. Franger, F.L. Cras, C. Bourbon, H. Rouault, J. Power Sources, **2003**, 119-121, 252.